

Validation of Novel 3-Dimensional Electrocardiographic Mapping of Atrial Tachycardias by Invasive Mapping and Ablation

A Multicenter Study

Ashok J. Shah, MD,* Meleze Hocini, MD,* Olivier Xhaet, MD,* Patrizio Pascale, MD,* Laurent Roten, MD,* Stephen B. Wilton, MD, PhD,* Nick Linton, MD, PhD,* Daniel Scherr, MD,* Shinsuke Miyazaki, MD,* Amir S. Jadidi, MD,* Xingpeng Liu, MD,* Andrei Forclaz, MD,* Isabelle Nault, MD,* Lena Rivard, MD,* Michala E. F. Pedersen, MD, PhD,* Nicolas Derval, MD,* Frederic Sacher, MD,* Sebastien Knecht, MD, PhD,* Pierre Jais, MD,* Remi Dubois, PhD,* Sandra Eliautou, PhD,* Ryan Bokan, BSE,† Maria Strom, PhD,† Charu Ramanathan, PhD,† Ivan Cakulev, MD,‡ Jayakumar Sahadevan, MD,‡ Bruce Lindsay, MD,§ Albert L. Waldo, MD,‡ Michel Haissaguerre, MD*

Bordeaux, France; and Cleveland, Ohio

Objectives

This study prospectively evaluated the role of a novel 3-dimensional, noninvasive, beat-by-beat mapping system, Electrocardiographic Mapping (ECM), in facilitating the diagnosis of atrial tachycardias (AT).

Background

Conventional 12-lead electrocardiogram, a widely used noninvasive tool in clinical arrhythmia practice, has diagnostic limitations.

Methods

Various AT (de novo and post-atrial fibrillation ablation) were mapped using ECM followed by standard-of-care electrophysiological mapping and ablation in 52 patients. The ECM consisted of recording body surface electrograms from a 252-electrode-vest placed on the torso combined with computed tomography-scan-based biatrial anatomy (CardioInsight Inc., Cleveland, Ohio). We evaluated the feasibility of this system in defining the mechanism of AT—macro-re-entrant (perimitral, cavotricuspid isthmus-dependent, and roof-dependent circuits) versus centrifugal (focal-source) activation—and the location of arrhythmia in centrifugal AT. The accuracy of the noninvasive diagnosis and detection of ablation targets was evaluated vis-à-vis subsequent invasive mapping and successful ablation.

Results

Comparison between ECM and electrophysiological diagnosis could be accomplished in 48 patients (48 AT) but was not possible in 4 patients where the AT mechanism changed to another AT (n = 1), atrial fibrillation (n = 1), or sinus rhythm (n = 2) during the electrophysiological procedure. ECM correctly diagnosed AT mechanisms in 44 of 48 (92%) AT: macro-re-entry in 23 of 27; and focal-onset with centrifugal activation in 21 of 21. The region of interest for focal AT perfectly matched in 21 of 21 (100%) AT. The 2:1 ventricular conduction and low-amplitude P waves challenged the diagnosis of 4 of 27 macro-re-entrant (perimitral) AT that can be overcome by injecting atrioventricular node blockers and signal averaging, respectively.

Conclusions

This prospective multicenter series shows a high success rate of ECM in accurately diagnosing the mechanism of AT and the location of focal arrhythmia. Intraprocedural use of the system and its application to atrial fibrillation mapping is under way. (J Am Coll Cardiol 2013;62:889–97) © 2013 by the American College of Cardiology Foundation

From the *Department of Rhythmologie, Hôpital Cardiologique du Haut-Lévêque and the Université Bordeaux II, Bordeaux, France; †Division of Scientific Affairs, CardioInsight Technologies, Cleveland, Ohio; ‡Division of Cardiovascular Medicine, Harrington Heart and Vascular Institute, University Hospitals Case Medical Center and Case Western Reserve University, Cleveland, Ohio; and the §Section of Cardiac Electrophysiology, Department of Cardiovascular Medicine, Cleveland Clinic, Cleveland, Ohio. The research leading to these results has received funding from the European Union Seventh Framework Programme (FP7/2007-2013) under Grant Agreement HEALTH-F2-2010-261057. Drs. Hocini, Jais, and Haissaguerre are

stockowners in CardioInsight Inc. Dr. Dubois is a paid consultant to and stockowner in CardioInsight Inc.; and has received unrestricted research grants from Sorin. Dr. Eliautou is a paid consultant to CardioInsight Inc. Mr. Bokan and Drs. Strom and Ramanathan are paid employees and stockowners in CardioInsight Inc. Drs. Lindsay and Waldo are members of the scientific advisory board of and have received honoraria from CardioInsight Inc. All other authors have reported that they have no relationships relevant to the contents of this paper to disclose.

Manuscript received September 17, 2012; revised manuscript received February 21, 2013, accepted March 12, 2013.

**Abbreviations
and Acronyms****3D** = 3-dimensional**AF** = atrial fibrillation**AT** = atrial tachycardia(s)**CT** = computerized
tomography**ECG** = electrocardiography**ECM** = Electrocardiographic
Mapping**EP** = electrophysiological

Atrial tachyarrhythmias (AT) represent the most common clinical heart rhythm disorder (1). The management of AT, including those arising in patients undergoing atrial fibrillation (AF) (2) ablation, is challenging due to various mechanisms and ubiquitous locations. Twelve-lead electrocardiography (ECG) is the standard-of-care technology to diagnose the origin and mechanism of atrial tachyarrhythmia arising in

patients with or without previous ablation prior to clinical cardiac electrophysiological (EP) intervention (3,4). However, the 12-lead ECG is limited in diagnosing the mechanisms and localization of the arrhythmias, particularly in the setting of previous ablation and often requires complicated algorithms (5).

See page 898

With the advent of percutaneous transvascular catheterization and electrical mapping systems in the EP lab, it has become possible to simultaneously evaluate, diagnose, and treat the arrhythmias. In the last 2 decades, technological advances have resulted in the development of multiple, sophisticated, high-density and/or 3-dimensional (3D) mapping systems for the diagnosis and understanding of different types of atrial arrhythmias (6,7). These have helped to improve existing and evolve novel approaches to treat simple and complex atrial rhythm disorders. However, most advanced mapping systems rely on serial, beat-by-beat arrhythmia mapping, which requires 10 to 30 min for acquisition and additional post-processing to understand the mechanism of AT. In addition, these systems provide mapping information only during the invasive procedure; thereby, they are lacking the advantage of allowing physicians to plan the procedure in advance for better management of complex arrhythmia. Therefore, diagnosing AT may be a challenge, leaving room for improvement in planning invasive EP study and subsequent ablation.

Electrocardiographic mapping (ECM) is a novel 3D, 252-lead, surface ECG-based noninvasive epicardial mapping system that provides global chamber mapping in a single beat (8,9). We aim to evaluate the potential of this mapping system in a series of patients with AT arising in various clinical settings.

Methods

Study population. Fifty-two patients with clinical AT (including post-AF ablation and post-atriotomy) from 3 centers (in France and the United States) consented to participate in the study, which was approved by the institutional review committees of all the participating centers. All patients underwent the ECM procedure (CardioInsight Inc., Cleveland, Ohio). The accuracy of the system in diagnosing the arrhythmia mechanism

and location of arrhythmia during AT was determined by comparison with invasive mapping and confirmed by successful ablation in all patients. Invasive EP mapping was performed using conventional electrogram and 3D electroanatomical mapping system (Carto XP, Biosense Webster, Diamond Bar, California; or NavX, St. Jude Medical Inc., Minneapolis, Minnesota) guidance. ECM was considered accurate when the detection of the clinical target by ECM matched with that obtained on invasive EP mapping and subsequently confirmed by successful ablation. A schema of biatrial anatomy was prepared based on biatrial epicardial geometry obtained from a computed tomography scan. The schematic was divided into 20 anatomical segments (Online Fig. 1). The segmentwise location of the source of each centrifugal AT was indicated on the schematic. Similarly, the macro-re-entrant AT involving 3 or more contiguous segments were represented by drawing the tachycardia circuit on the schematic.

Electrocardiographic mapping. The signal acquisition from the patient and subsequent computational methods used in the reconstruction of ECM maps using multiple torso electrodes have been previously described (8). Briefly, a 252-electrode vest is applied to the patient's torso and connected to the ECM system and surface potentials are recorded. It is followed by a noncontrast thoracic computed tomography scan to obtain high-resolution images of the heart and the vest electrodes. The electrode positions and 3D epicardial biatrial geometry are obtained via segmentation from the computed tomography images. The system reconstructs epicardial potentials and unipolar electrograms from torso potentials during each beat per cycle using mathematical reconstruction algorithms. Details of the mathematical methods have been provided in previous publications (9,10). Activation maps are computed using traditional unipolar electrogram intrinsic deflection-based ($-dV/dT_{max}$) method. In addition, a novel directional activation map using electrogram morphology and local propagation between adjacent electrograms facilitated the analysis of ECM.

All ECM data were analyzed by 2 operators systematically in a stepwise manner as follows:

1. A window of 1 tachycardia cycle involving distinct tachycardia P waves and/or the tachycardia-initiating beat, if available, was selected. The window was selected such that the beginning coincided with the predominant deflection on the body surface signal in the relative location of the anterior precordial leads. If additional cycles were available, signal averaging and specific algorithm-based analyses were undertaken.
2. Between the two atria, we grossly identified and distinguished the passively activated atrium (positive morphology [R or Rs] of unipolar electrograms) from the active (driving) chamber (negative morphology [QS or Qr] of unipolar electrograms) based on the selected window of interest.
3. The tachycardia mechanism was defined as “macro-re-entrant” (which includes perimitral, cavotricuspid isthmus-dependent, roof-dependent, and around surgical

scar tachycardias) or “centrifugal.” In centrifugal AT, the location of arrhythmia source was determined. In general, if an activation map of AT encompassed >75% of the cycle spread over 3 or more atrial segments in a re-entrant fashion around a large central obstacle, then the AT was diagnosed as macro-re-entrant. On the other hand, focal AT were diagnosed based on the presence of centrifugal spread of activation from small source (focus) (11).

Invasive EP study. After pre-procedural ECM, all the patients were subjected to invasive EP study. The invasive operator was blinded to the noninvasive diagnosis. Two or 3 vascular sheaths were inserted into the right femoral vein under lignocaine/bupivacaine local anesthesia. A steerable decapolar catheter (5 mm interelectrode spacing, Xtrem, Sorin Medical, Montrouge, France) or octapolar catheter (2-5-2 mm, EPXT, Bard Electrophysiology, Lowell, Massachusetts) was placed in the coronary sinus. Access into the left atrium, whenever required, was gained with trans-septal puncture (Adult BRK 71-cm needle, St. Jude Medical) using fluoroscopic and hemodynamic (pressure) guidance and confirmed by left atrial contrast atriogram. A 2-in-1 technique was used to pass a long sheath (St. Jude Medical SL0, 63-cm) and a 3.5-mm open-irrigated-tip catheter (ThermoCool D/F curve, Biosense Webster) across the septum into the left atrium via a single puncture. The long sheath was continuously perfused with heparinized saline at 100 to 200 ml/h. Following the completion of transseptal access, a weight-based bolus dose of unfractionated heparin was administered. The participating centers followed their institutional protocol to maintain adequate anticoagulation guided by activated clotting time (250 s, 350 to 400 s).

Sedation (level 3 on Ramsay sedation scale) and analgesia was determined by hospital protocol and consisted of: 1) midazolam, 0.02 mg/kg prior to femoral puncture; 2) morphine sulfate, 0.1 mg/kg pre-procedurally up to a maximum of 0.2 mg/kg or fentanyl 50 µg bolus with or without 3) supplementary analgesia (sufentanil) provided under anesthetic supervision. Monitoring with noninvasive blood pressure, digital pulse oximetry, and/or CO₂ end tidal volume was performed continuously throughout the procedure. Surface electrocardiograms and bipolar intracardiac electrograms were continuously monitored with the use of Lab System Pro (Bard Electrophysiology) or Cardiolab System (GE Medical Systems, Milwaukee, Wisconsin). Signals were sampled at 1 kHz and filtered at 0.1 to 50 Hz for surface electrocardiograms and 30 to 250 Hz for intracardiac signals.

Ablation parameters. Ablation was performed using a 3.5-mm externally irrigated-tip catheter (Thermocool, Biosense-Webster). The ablation parameters were regulated depending upon the site of ablation. In general, power delivery ranged from 20 to 35 W with target temperature usually below 43°C (maximum 45°C) achieved using manually adjustable irrigation rates of 5 to 60 ml/min (0.9% normal saline via a Cool Flow pump) (Biosense Webster, Diamond Bar, California) or with a fixed flow rate of 17 ml/min. The

Table 1 Baseline Characteristics (N = 52)

Age, yrs	61 ± 11
Sex	
Male	42 (81)
Female	10 (19)
Hypertension	16 (31)
Diabetes	06 (12)
Cerebrovascular accident	04 (08)
Structural heart disease	18 (35)
Antiarrhythmic drugs attempted, per patient	1.2 ± 0.9
Previous AF ablation	27 (52)
Linear lesions	14 (52)
Left atrial dimension, mm	43 ± 5
Left ventricular ejection fraction, %	52 ± 14
Atrial tachycardia cycle length, ms	284 ± 85

Values are mean ± SD or n (%).

AF = atrial fibrillation.

endpoint was termination of tachycardia during ongoing ablation. In patients who underwent pulmonary vein isolation previously, complete electrical isolation of all pulmonary veins was ensured before the end of the procedure and additional ablation was performed, if required. If linear lesions were deployed and gaps were discovered, further ablation was undertaken in paced/sinus rhythm until bidirectional block was ascertained.

Statistical analysis. Continuous data are reported as mean ± SD and categorical data are reported as percentages (Microsoft Excel software, Microsoft Corporation, Redmond, Washington).

Results

Baseline characteristics. The baseline clinical characteristics of 52 patients are provided in Table 1. The mean age was

Table 2 Accuracy of Electrocardiomapping in Defining Ablation Targets

Electrophysiological Laboratory Diagnosis	n	Previous AF Ablation	ECM Correctly Diagnosed	Diagnostic Accuracy, %
Re-entry				
Cavotricuspid isthmus-dependent	18	2	18	100
Roof-dependent	3	3	3	100
Perimitral	5	5	1	20
Around the scar	1	0	1	100
Total	27	10	23	85
Focal				
Right atrial	4	2	4	100
Left atrial	15	11	15	100
Septal	2	0	2	100
Total	21	13	21	100
Subtotal	48	23	44	92
Inevaluable	4	4	—	—
Grand total	52	27	—	—

Accuracy for unablated atria: 100% (25 of 25); accuracy for previously ablated atria: 83% (19 of 23).

AF = atrial fibrillation; ECM = electrocardiomapping.

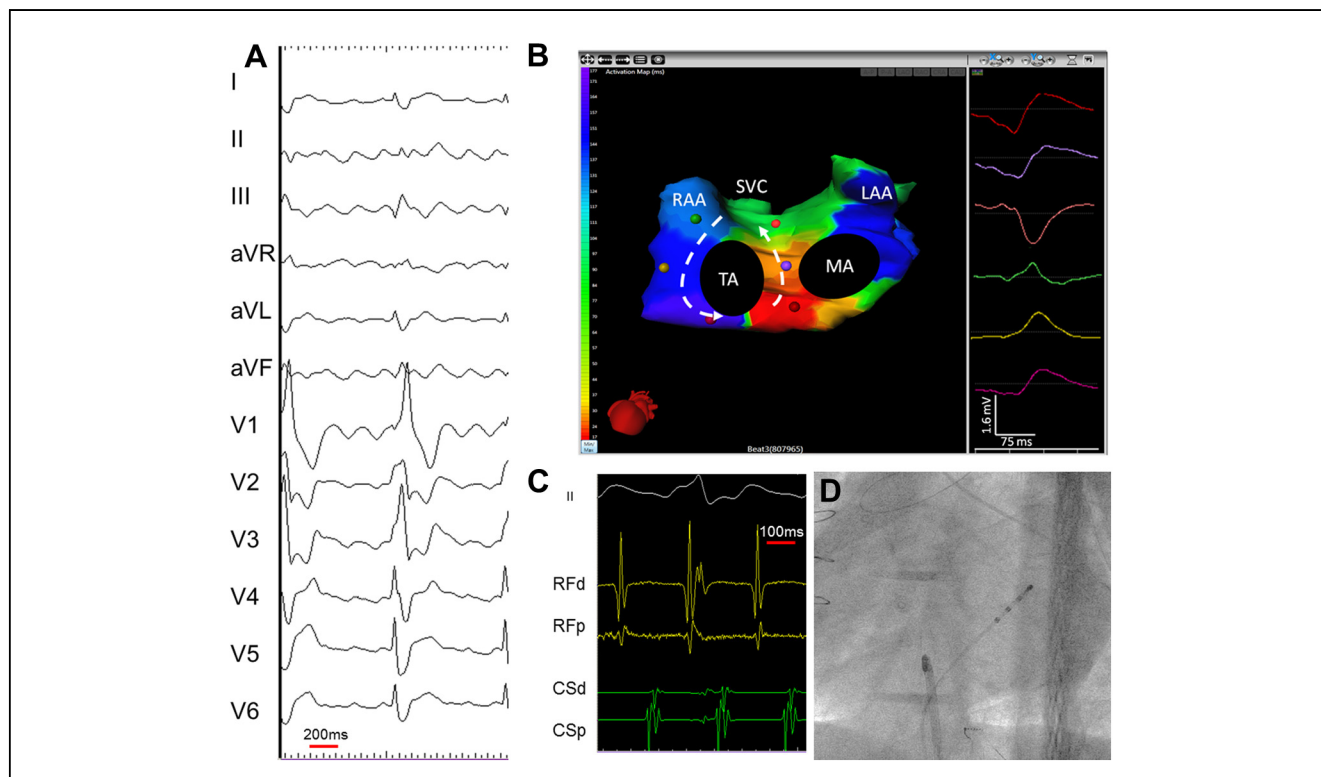


Figure 1 Cavotricuspid Isthmus-Dependent AT

(A) A 12-lead electrocardiogram of clinical tachycardia from a patient who previously underwent extensive ablation for atrial fibrillation. (B) An isochronal activation electrocardiogram of counterclockwise cavotricuspid isthmus-dependent atrial tachycardia (AT). Typically, the interatrial groove is activated from below upward followed by sequential activation of the right atrial free wall from above downward. The left atrial breakthroughs at the coronary sinus and the Bachmann bundle area result in septal-to-lateral activation of the anterior and posterior left atrium. The morphology of the virtual unipolar electrograms displayed on 6 atrial sites distributed around the tricuspid annulus concurs with this activation pattern. The color of the unipolar electrogram corresponds to the color of the spot marked on the biatrial geometry. [Online Video 1](#) shows an isopotential map of this AT. On the color scale, the earliest activation site is red and the latest is purple. The color map shows 160 ms of activation. The cycle length here is 244 ms. The remainder of the cycle length is within the slow conduction zone (cavotricuspid isthmus), on either side of which purple meets red. (C) Intracardiac electrograms from the isthmus and coronary sinus recorded during the ablation of cavotricuspid isthmus-dependent AT. (D) Postero-anterior fluoroscopic image showing the location of intracardiac catheters. LAA = left atrial appendage; MA = mitral annulus; RAA = right atrial appendage; SVC = superior vena cava; TA = tricuspid annulus.

61 ± 11 years and there were 42 male patients. Structural heart disease was present in 18 (35%), and 27 (52%) patients had previous AF ablation (including surgical ablation in 1 patient). Two patients had undergone bilateral lung transplantation. The mean cycle length of the clinical AT was 284 ± 85 ms.

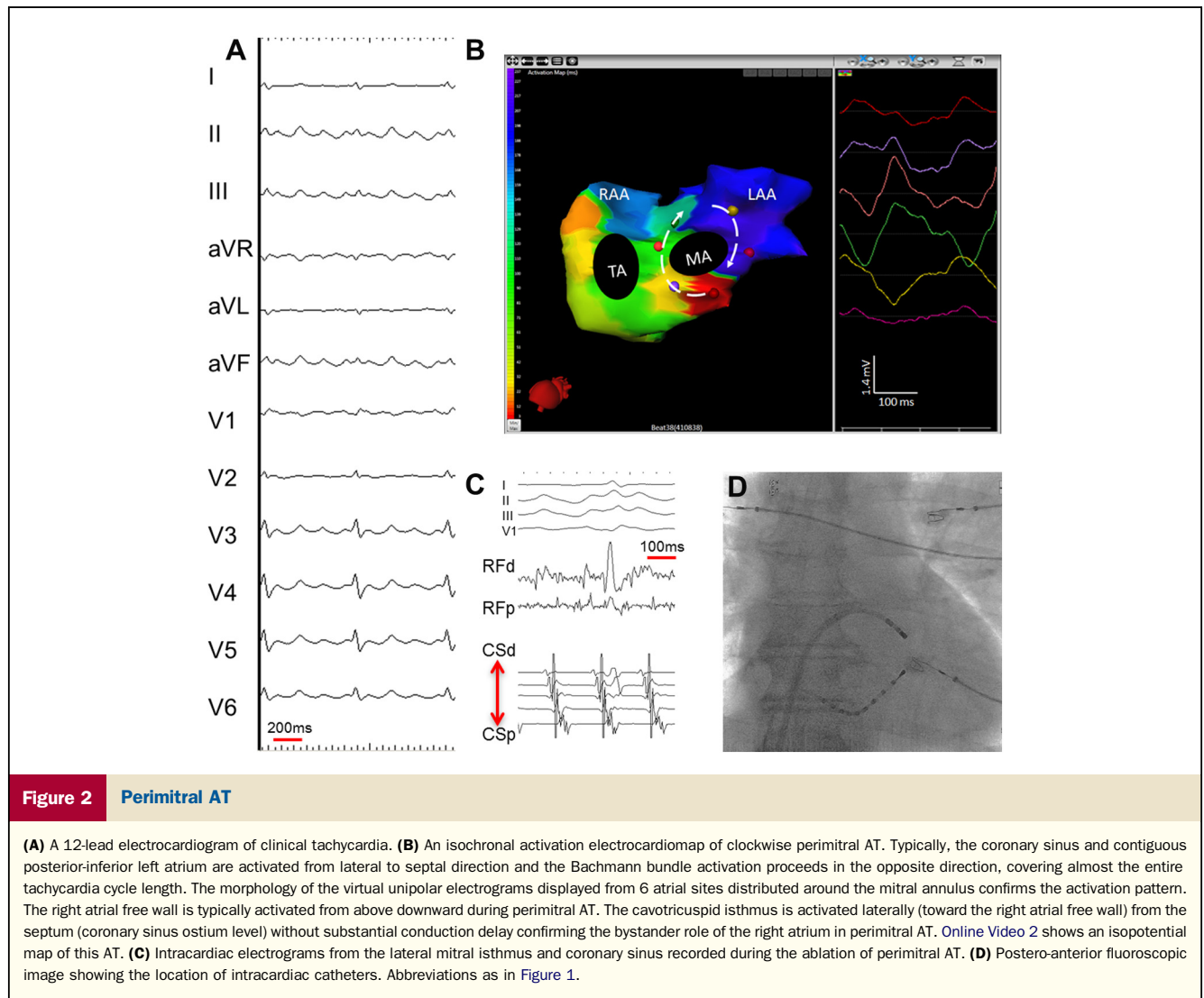
Electrophysiological diagnosis. All patients were first mapped at the bedside using ECM, followed median 1 day (interquartile range 1 to 7) after by invasive mapping and ablation. In the majority of patients, the system processed the data and generated the maps in less than 5 min. The ECM diagnosis was evaluable in 48 of 52 patients in whom there was confirmed EP diagnosis and successful ablation. In 4 patients, clinical AT converted to another rhythm (AT and AF in 1 each and sinus in 2) before invasive mapping was completed, and therefore, these patients were excluded from the comparative analysis ([Table 2](#)).

Types of atrial tachycardia. Out of 48 evaluable clinical AT, 27 AT were diagnosed in the EP laboratory as macro-re-entrant and 21 as centrifugal arrhythmias ([Online Fig. 2](#)). All of them were successfully terminated by ablation resulting in sinus

rhythm in 44 or to another AT in 4. ECM identified the mechanism of AT as macro-re-entry versus centrifugal activation in 44 of 48 (92%) patients ([Table 2](#)).

RE-ENTRANT ATRIAL TACHYCARDIA. Among 27 re-entrant AT diagnosed invasively, there were 18 cavotricuspid isthmus-dependent, 5 perimitral, and 3 roof-dependent AT ([Figs. 1 to 3](#), respectively; see also [Online Videos 1, 2, and 3](#)). Additionally, 1 AT was a re-entry around the right atrial post-atriotomy scar ([Online Fig. 2](#)). Ten of 27 (37%) re-entrant ATs (5 perimitral, 3 roof-dependent, and 2 cavotricuspid isthmus-dependent AT) were observed in patients who had had previous AF ablation (including linear lesions in 7 patients).

Overall, ECM accurately diagnosed 85% of the re-entrant AT. The diagnostic accuracy of ECM for the cavotricuspid isthmus- and roof-dependent AT and the post-atriotomy scar-related AT was found to be 100%. One of 5 perimitral AT cases was diagnosed accurately on ECM. In the rest, no definite pattern (focal or re-entry) emerged on the analysis of ECM during AT except for counterclockwise (superior to inferior)



activation of right atrial lateral wall. These were our initial cases where QRST-complex superimposition on P waves (2:1 atrio-ventricular conduction) disallowed selection of 1 full tachycardia cycle. This could have been potentially resolved by slowing the ventricular rate. In addition, these were also the post-ablation atria with substantially low tachycardia P-wave amplitudes, which further complicated and challenged the diagnosis. The median value of the invasive bipolar voltages in the region of the coronary sinus was 0.2 mV (range 0.05 to 3.53 mV) ([Online Fig. 3](#)).

CENTRIFUGAL ATRIAL TACHYCARDIA. As described, all focal AT were diagnosed based on the presence of centrifugal spread of activation from a small source (11). Among 21 centrifugal AT ([Table 2](#)), 15 originated from the left atrium ([Fig. 4](#)), 4 from the right ([Fig. 5](#)), and 2 from interatrial septum ([Online Fig. 4](#)). The atrial distribution of the centrifugal sites is illustrated in [Online Figure 2](#). Thirteen (62%) centrifugal AT were associated with previous AF ablation.

Left atrium source. ECM correctly diagnosed all left atrial centrifugal AT. Among the 7 AT originating anteriorly in the left atrium, 3 originated from the anterior wall, 2 from the appendage, 1 from the junction of the left atrium and the appendage, and 1 from the anterior left superior pulmonary venous ostial region. Among the 8 AT originating posteriorly in the left atrium, 5 were located at the pulmonary venous ostia (left superior: 2, right superior: 1, left inferior: 1, right inferior: 1), 1 on the roof, 1 at the junction of roof with right superior pulmonary venous ostium, and 1 on the posterior wall at the site of left inferior vein suture in a patient with bilateral pulmonary transplant.

Right atrium source. ECM correctly diagnosed all right atrial centrifugal AT. Among 4 right atrial sources, 1 AT originated below the location of the sino-atrial node posteriorly, 1 from the ostial superior vena cava, 1 from the cavotricuspid isthmus, and 1 anterolaterally in the free wall ([Fig. 5](#)).

Interatrial septum source. Between the 2 septal centrifugal AT diagnosed on ECM, 1 arose from the septum near the fossa

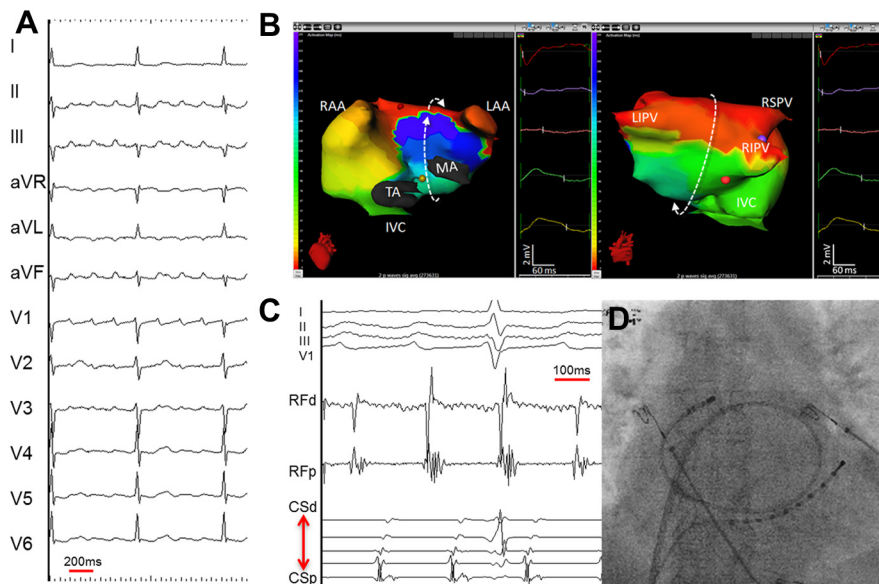


Figure 3 Left Atrial Roof-Dependent AT

(A) A 12-lead electrocardiogram of clinical tachycardia. (B) An isochronal activation electrocardiogram map of a typical macro-re-entrant roof-dependent AT. The below upward activation of the anterior wall of the left atrium is shown on the left and the top to bottom activation of the posterior left atrium is shown on the right. The bystander right atrial free wall is activated from above downward. The entire tachycardia cycle length is covered along the AT circuit and the morphology of the virtual unipolar electrograms displayed from 5 atrial sites distributed along the trajectory of the macro-re-entry concur with this activation pattern. [Online Video 3](#) shows an isopotential map of this AT. (C) Intracardiac electrograms from the left atrial roof and coronary sinus recorded during the ablation of roof-dependent AT. (D) Postero-anterior fluoroscopic image showing the location of intracardiac catheters. IVC = inferior vena cava; LIPV = left inferior pulmonary vein; RIPV = right inferior pulmonary vein; RSPV = right superior pulmonary vein; other abbreviations as in [Figure 1](#).

ovalis, and 1 from the superior left atrial septum. Whereas the source was not directly visualized on the biatrial map, a septal mechanism was deduced from the earliest epicardial exit, which was observed at the anterior interatrial groove. An example is shown in [Online Figure 4](#), where an inferior interatrial groove breakthrough occurs 11 ms after the P-wave onset, and this is followed within a short interval (27 ms) by a superior atrial roof breakthrough due to the septal focal wave front propagating superiorly through the septum. ECM correctly diagnosed both septal centrifugal AT.

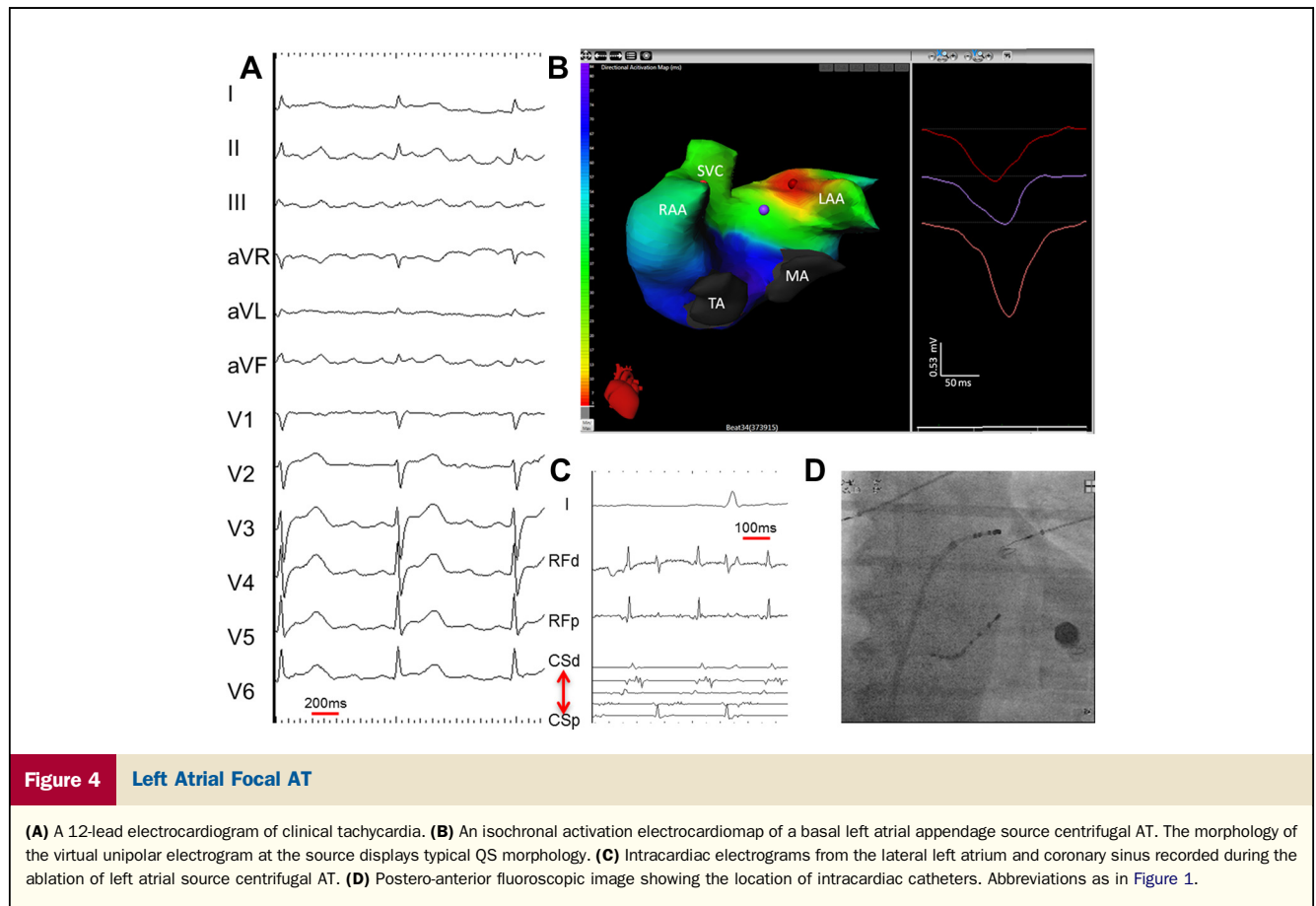
PREVIOUS ABLATION PROCEDURE AND ECM ACCURACY. The diagnostic accuracy of ECM in patients with previous AF ablation was 83% (19 of 23 AT). In the remaining 25 cases without any previous atrial ablation, the diagnosis was accurately obtained in 25 of 25 AT (100%). Two septal-source centrifugal AT, each of which presented with epicardial exit on the anterior interatrial groove, were also accurately diagnosed by ECM.

Discussion

The ECM technology has been used in noninvasively reconstructing the electrophysiological properties of the heart in structurally normal and diseased hearts (12–16). In this study, we demonstrate the clinical utility of this external, single-beat 3D mapping system in mapping simple and

complex AT. The overall diagnostic accuracy of ECM compared with invasive EP diagnosis, as the gold standard, was 92% (100% in patients with de novo ablations and 83% in patients with previous AF ablations). ECM was particularly useful and adept at accurately diagnosing centrifugal AT in 100% of patients, including 13 (62%) patients with previous AF ablation. Among the patients with centrifugal AT, differentiation of true focal from localized (not macro) re-entrant AT could not be established. Whereas such differentiation may be important from a mechanistic perspective, it is irrelevant for identifying the clinical ablation target (17).

Initially in this study, it was challenging to map 4 cases of perimitral AT. The 2 primary reasons for failure were: 1) the 2:1 atrioventricular conduction, precluding selection of a full tachycardia cycle (unmasked by QRST complex); and 2) addition to low-voltage electrograms. Noise reduction using a signal-averaging algorithm was very practical and clinically useful for stable monomorphic arrhythmias without altering the morphology or frequency content of low-amplitude signals by traditional filtering techniques. Signal averaging could not be employed when the QRST complex obscured the P waves. However, there are known signal-processing techniques that can be incorporated to remove the ventricular complex from obscuring the P waves, and these warrant further development. Alternatively, administration

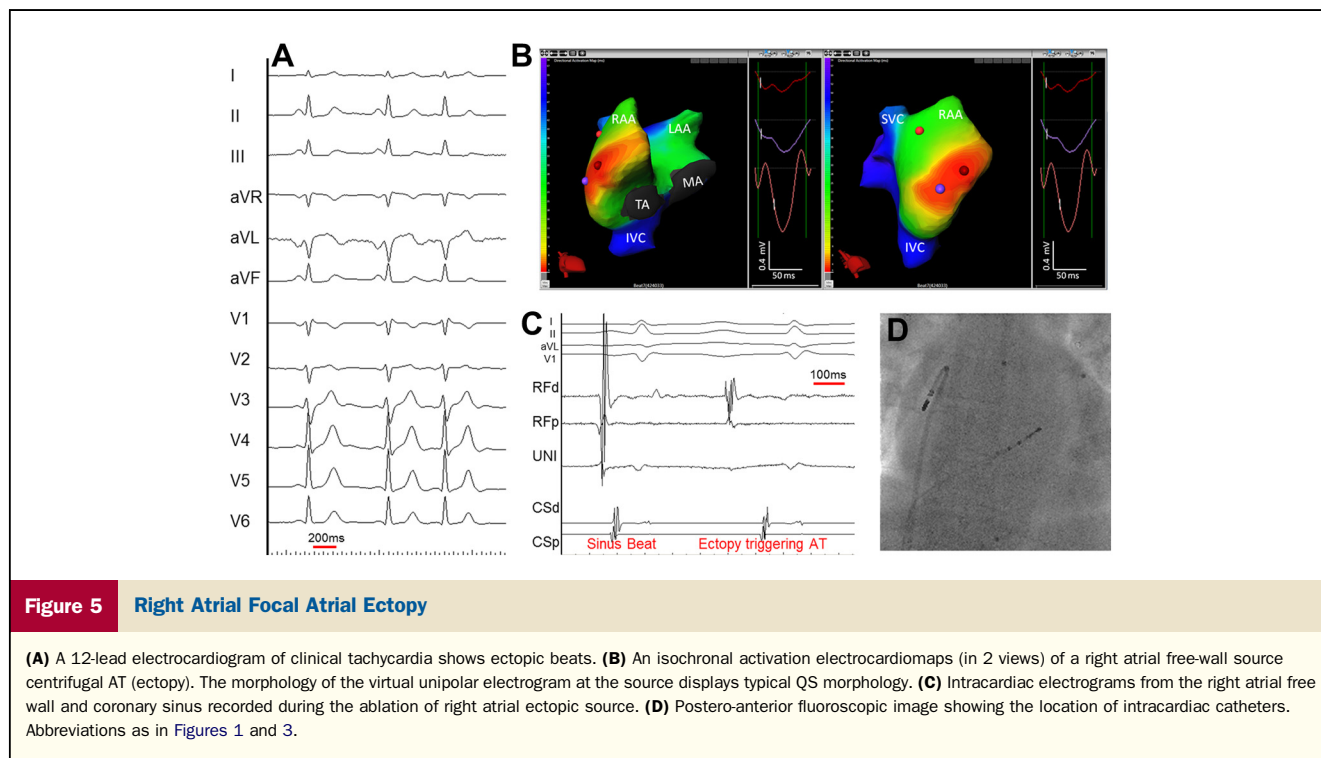


of atrioventricular node blockers or simple pacing maneuvers during the invasive procedure can unmask the P waves (i.e., post-ventricular pacing pause in the R-R interval can allow unobscured (by QRST complex) P waves or multiple AT cycle capture). In our recent experience with per procedural use of the system, we have been successful in diagnosing several clockwise and counterclockwise perimitral AT cases with and without simultaneous roof-dependent circuits using long R-R intervals, signal average, and other noise-filtering techniques despite low-amplitude P waves from extensive atrial ablation.

Study limitations. First, the system is not able to provide direct mapping of the septum. Because the septum is not an epicardial structure and therefore not included or displayed on the map, a septal source can be deduced by analyzing the location (interatrial groove) and timing of the epicardial breakthrough. Second, ECM provides epicardial maps. Although there is experimental evidence for differential activation of the contiguous endo-epicardium in the atria (in at least some of its parts), the difference may be considered modest, at best, or even negligible in this multicenter study, where there was virtually no difference between the epicardial ECM and endocardial targets of ablation, as evidenced in [Online Figure 5](#) and previously published reports (12,13). Indeed, the atrial tissue is much thinner (in most parts)

than the ventricular myocardium is, and evaluating the quantitative resolution of the system was beyond the scope of this study. Third, AT with 2:1 conduction to the ventricles pose an analytic challenge in the absence of reliable QRST-subtraction software program. The use of atrioventricular node blockers is strongly recommended in this situation. Fourth, AT with low signal-to-noise ratio may be challenging to analyze. Further development of signal processing techniques, including averaging and appropriate filtering, has helped improve the accuracy of diagnosis in such situations as successfully evaluated in successive patients.

Clinical perspectives. First, ECM is a novel tool that noninvasively provides global atrial activation patterns of sustained as well as transient AT from a single tachycardia beat per cycle. On the other hand, current sequential beat mapping techniques necessitates sustenance of AT or repetitive occurrence of ectopic beats, making the approach impractical in nonsustained AT. Single-beat, simultaneous mapping can be crucial when the clinical AT frequently changes from 1 form to another and back and also for mapping the beats, which trigger sustained arrhythmias such as AF. Such a beat-to-beat analysis allows tracking of the changes, which may arise spontaneously or after ablation. Being a noninvasive system, ECM is a mapping technology that can be applied bedside, potentially providing the EP



physician with more data to plan the ablation procedure. Quantification of the clinical impact of ECM in saving procedure time, fluoroscopic exposure, and, in general, the efficacy of the ablation procedure is a logical next step. Second, real-time panoramic mapping, progress in computer technology, and new signal processing will add further advantages over conventional ECG and enhance the utility of the current system beyond global atrial activation and tissue-level information like local electrograms (i.e., morphology) and voltage.


Conclusions

This multicenter experience with novel, noninvasive mapping system in a wide range of patients demonstrates the feasibility of accurately identifying the atria where the AT is located and defining the AT mechanism. This study demonstrates the clinical utility of the system in the noninvasive diagnosis of various atrial tachycardias. The rapid (single beat per cycle) mapping and reliable diagnostic ability of the system underscore its potential to reduce ablation and procedural times and suggests its potential role in mapping rapidly changing arrhythmias such as AF.

Reprint requests and correspondence: Dr. Ashok J. Shah, Service de Rythmologie, Hôpital Cardiologique du Haut-Lévêque, Avenue de Magellan, 33604 Bordeaux-Pessac, France. E-mail: drashahep@gmail.com.

REFERENCES

- Go AS, Hylek EM, Phillips KA, et al. Prevalence of diagnosed atrial fibrillation in adults: national implications for rhythm management and stroke prevention: the Anticoagulation and Risk Factors in Atrial Fibrillation (ATRIA) Study. *JAMA* 2001;285:2370–5.
- Deisenhofer I, Estner H, Zrenner B, et al. Left atrial tachycardia after circumferential pulmonary vein ablation for atrial fibrillation: incidence, electrophysiological characteristics, and results of radiofrequency ablation. *Europace* 2006;8:573–82.
- Gerstenfeld EP, Dixit S, Bala R, et al. Surface electrocardiogram characteristics of atrial tachycardias occurring after pulmonary vein isolation. *Heart Rhythm* 2007;4:1136–43.
- Brown JP, Krummen DE, Feld GK, Narayan SM. Using electrocardiographic activation time and diastolic intervals to separate focal from macro-re-entrant atrial tachycardias. *J Am Coll Cardiol* 2007;49:1965–73.
- Jaïs P, Matsuo S, Knecht S, et al. A deductive mapping strategy for atrial tachycardia following atrial fibrillation ablation: importance of localized reentry. *J Cardiovasc Electrophysiol* 2009;20:480–91.
- Dong J, Zrenner B, Schreieck J, et al. Catheter ablation of left atrial focal tachycardia guided by electroanatomic mapping and new insights into interatrial electrical conduction. *Heart Rhythm* 2005;2:578–91.
- Gaita F, Calò L, Riccardi R, et al. Different patterns of atrial activation in idiopathic atrial fibrillation: simultaneous multisite atrial mapping in patients with paroxysmal and chronic atrial fibrillation. *J Am Coll Cardiol* 2001;37:534–41.
- Oster HS, Taccardi B, Lux RL, Ershler PR, Rudy Y. Noninvasive electrocardiographic imaging: reconstruction of epicardial potentials, electrograms, and isochrones and localization of single and multiple electrocardiac events. *Circulation* 1997;96:1012–24.
- Ramanathan C, Ghanem RN, Jia P, Ryu K, Rudy Y. Noninvasive electrocardiographic imaging for cardiac electrophysiology and arrhythmia. *Nat Med* 2004;10:422–8.
- Rudy Y, Burnes JE. Noninvasive electrocardiographic imaging. *Ann Noninvasive Electrocardiol* 1999;4:340–59.
- Saoudi N, Cosio F, Waldo A, et al. Classification of atrial flutter and regular atrial tachycardia according to electrophysiologic mechanism

- and anatomic bases: a statement from a joint expert group from the Working Group of Arrhythmias of the European Society of Cardiology and the North American Society of Pacing and Electrophysiology. *J Cardiovasc Electrophysiol* 2001;12:852–66.
12. Ghanem RN, Jia P, Ramanathan C, Ryu K, Markowitz A, Rudy Y. Noninvasive electrocardiographic imaging (ECGI): comparison to intraoperative mapping in patients. *Heart Rhythm* 2005;2:339–54.
 13. Intini A, Goldstein RN, Jia P, et al. Electrocardiographic imaging (ECGI), a novel diagnostic modality used for mapping of focal left ventricular tachycardia in a young athlete. *Heart Rhythm* 2005;2: 1250–2.
 14. Wang Y, Cuculich PS, Woodard PK, Lindsay BD, Rudy Y. Focal atrial tachycardia after pulmonary vein isolation: noninvasive mapping with electrocardiographic imaging (ECGI). *Heart Rhythm* 2007;4:1081–4.
 15. Wang Y, Schuessler RB, Damiano RJ, Woodard PK, Rudy Y. Noninvasive electrocardiographic imaging (ECGI) of scar-related atypical atrial flutter. *Heart Rhythm* 2007;4:1565–7.
 16. Cuculich PS, Wang Y, Lindsay BD, et al. Noninvasive characterization of epicardial activation in humans with diverse atrial fibrillation patterns. *Circulation* 2010;122:1364–72.
 17. Sanders P, Hocini M, Jaïs P, et al. Characterization of focal atrial tachycardia using high-density mapping. *J Am Coll Cardiol* 2005;46: 2088–99.
-
- Key Words:** ablation ■ atrial tachycardia ■ electrocardiographic mapping ■ noninvasive mapping.
-
-  **APPENDIX**
-
- For supplemental figures and videos, please see the online version of this article.**